

Treatment of Deliming-bating Effluent from Tannery using Membrane Separation Processes

Chandan Das, Sunando DasGupta and Sirshendu De*

Department of Chemical Engineering, Indian Institute of Technology, Kharagpur, Kharagpur - 721302, India

Abstract

A hybrid membrane separation process involving ultrafiltration and nanofiltration is investigated to treat deliming-bating effluent of a tannery. The pretreatment of the effluent is carried out by coagulation using alum. The optimum concentration of the alum is obtained as 2% (wt/vol). The effects of operating conditions *e.g.*, transmembrane pressure drop and cross flow velocity on the permeate flux and quality are observed by conducting the experiments in total recirculation mode. The effects of hydrodynamic conditions in the membrane channel on the system performance are also investigated by imposing laminar, laminar flow with turbulent promoter, and turbulent flow conditions. A resistance-in-series model is used to quantify the flux decline. Fertilizer value of the dried sludge is also evaluated and is found to be close to the quality of vermi compost.

Keywords: Ultrafiltration, nanofiltration, deliming-bating effluent, turbulent promoter, resistance-in-series model.

JEPS (2008), Vol. 2, pp. 11 – 24.

Introduction

In tannery, raw hides and skins are converted into leather by several unit operations, namely soaking, liming, deliming-bating, pickling, degreasing, tanning, dyeing, fatliquoring, *etc.* The second tannery operation is liming. Excess lime and other alkalis used in liming is removed either by repeated washing in water or by chemical treatment using acids and/or acidic salts or by both in deliming step. In the bating operation, the pelts are treated with a solution of proteolytic enzymes derived from fermented infusions of hen and pigeon dungs [1]. Therefore, deliming-bating operation results in huge amount of wastewater. A typical tannery generates around 450 m³ deliming-bating effluent per day. Around 75,000 m³/day liquid effluent is generated in India and 70,000 tonnes hides and skins are processed every year [2]. This wastewater can be further treated for safe disposal or recycled back to reduce the water and chemical consumption. Now a days it is preferred to treat the different waste water separately than mixing all the effluents [3]. Membrane based separation processes can be

attractive alternative in this regard. The major advantages of these processes include separation without any phase change and hence energy efficient. No additional chemicals are also required [4].

Cassano *et al.* [5] conceptualized various membrane separation processes involving ultrafiltration (UF), nanofiltration (NF) and reverse osmosis (RO) for the treatment of effluent emerging out from various unit operations of a tannery. They proposed UF to treat the deliming - bating effluent. In the treated effluent, COD and fatty acid are substantially reduced and the clear solution can be reused for preparation of bating bath or wash water. Some studies involving application of membrane based processes for treatment of effluent from various units of tannery are reported [6-8]. Recovery and reuse of chemicals in unhairing, degreasing and tanning processes by UF, NF and RO have been tested and the effects of membrane type, operating parameters have been discussed [9]. UF and NF are used in conjunction to treat the liming effluent [10, 11]. Application of UF and RO to the effluents from degreasing is also investigated [12, 13]. The common tannery effluent from all the steps, (*e.g.*, soaking, liming, deliming, bating, pickling, degreasing, *etc.*) except, chrome tanning is subjected to pretreatment procedures

*To whom all correspondence should be addressed: Tel: + 91-3222-283926; Fax: + 91-3222-255303; E-mail: sde@che.iitkgp.ernet.in (S. De)

followed by NF [2, 14]. In order to bring down the BOD and COD level below the permissible limit, the permeate solution of NF is further subjected to RO [2, 14]. Application of UF, NF and RO for recovery of chromium from tannery effluents is widely studied [15-19].

In the present study, an experimental scheme is formulated to treat the deliming-bating effluent using a hybrid process, including alum coagulation, ultrafiltration and nanofiltration. The optimum alum dose is found out. The fertilizer value of the produced sludge is evaluated. The supernatant liquor is subjected to cross flow ultrafiltration followed by nanofiltration in a continuous mode of operation. Effects of operating pressure and change in hydrodynamics (laminar, laminar with turbulent promoter and turbulent flow regime) on the permeate flux are observed. A resistance-in-series model is used to quantify the flux decline with a first order kinetic model for the growth of the polarized layer. The treatment performance is finally evaluated in terms of various properties like BOD, COD, TS, conductivity, *etc.* The proposed scheme of the treatment process is presented in Figure 1.

Theory

Flux decline analysis

The permeate flux at any point of time is expressed as,

$$v_w = \frac{\Delta P}{\mu[R_m + R_p(t)]} \quad (1)$$

where, R_m is the membrane resistance and R_p is the polarized layer resistance, which is a function of time. The development of polarized layer resistance is assumed to obey a first order kinetics as follows:

$$\frac{dR_p}{dt} \propto (R_p^s - R_p) \quad (2)$$

where, R_p^s is the steady state polarized layer resistance.

Eq. (2) can be written in the form as,

$$\frac{dR_p}{dt} = k(R_p^s - R_p) \quad (3)$$

where k is the first order rate constant. The above equation can be integrated with the initial condition, $R_p=0$ at $t=0$,

$$R_p = R_p^s[1 - \exp(-kt)] \quad (4)$$

Therefore, a plot of $\ln\left(\frac{R_p^s}{R_p^s - R_p}\right)$ versus time should be

a straight line passing through the origin with a slope equal to ' k '.

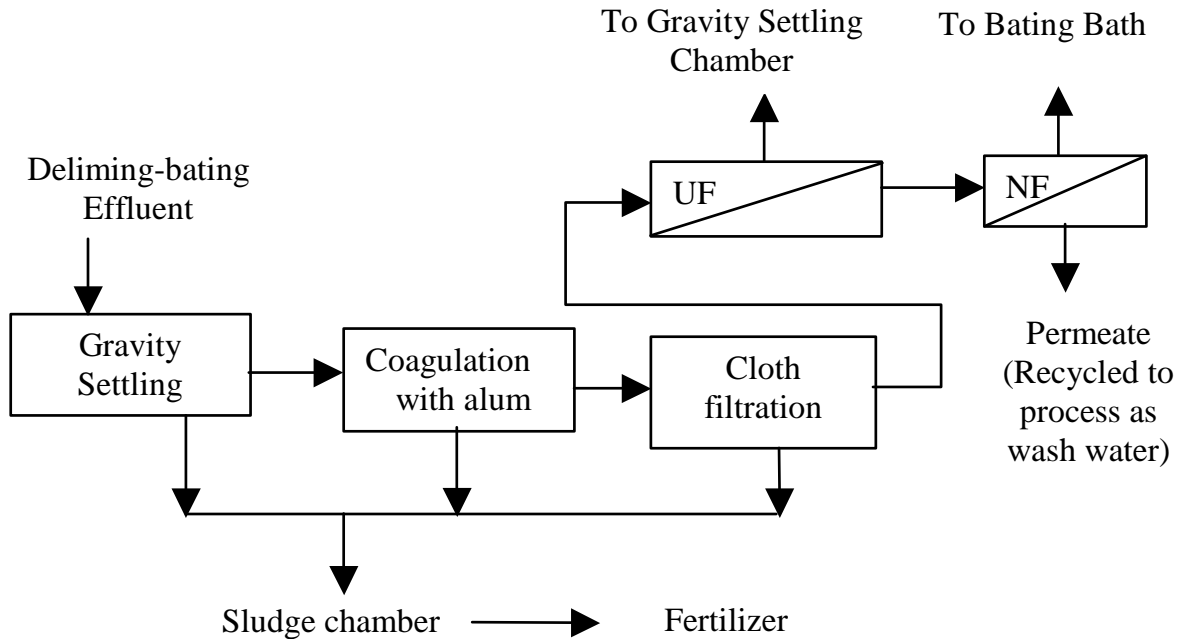


Figure 1. Proposed scheme for the treatment of deliming-bating effluent.

Experimental

Effluent

The delimiting-bating effluent is collected from M/s, Alison Tannery, Kolkata, India. The characterization of the effluent has been performed and the results are presented in Table 1.

Materials

Commercial potash alum is used for coagulation and is procured from the local market. All the chemicals, required for the determination of COD and BOD, are procured from Merck Limited, India and Loba Chemie, India and are of the analytical grade.

Membranes

Thin film composite (TFC) membranes are used for both ultrafiltration and nanofiltration. The hydraulic resistance of the UF membrane is $25.6 \times 10^{12} \text{ m}^{-1}$ with a molecular weight cut off of 5 kDa. The membrane is obtained from Permionics Membranes Pvt. Ltd., Gorwa, Vadodara, India. The hydraulic resistance of the NF membrane is $38.5 \times 10^{12} \text{ m}^{-1}$ with a molecular weight cut off of 400 Da. The membrane is supplied by M/s, Genesis Membrane Sepratech Pvt. Ltd., Mumbai, India.

Experimental Setup

Pretreatment

Coagulation study using commercial alum has been carried out in several graduated cylinders of 50 ml capacity with different dosages of alum.

Membrane cell

A rectangular cross-flow cell, made of stainless steel, is designed and fabricated. The cell consists of two rectangular matching flanges. The inner surface of the top flange is mirror polished. The bottom flange is grooved, forming the channels for the permeate flow. A porous stainless steel plate is placed on the lower plate that provides mechanical support to the membrane which is placed over the porous plate. Two silicon gaskets are placed over the membrane forming the flow channel.

For experiments with turbulent promoters, sixteen equispaced thin wires of diameter 0.19 mm are placed laterally (along the width of the channel) in between the two gaskets. The spacing between the turbulent promoters is 14.0 mm. The diameter, number and spacing between two promoters are optimized through a systematic experimental study [20]. The two flanges are tightened to create a leak proof channel. The effective length and width of the membrane available for filtration are 26.1 cm and 4.9 cm, respectively. The height of the flow channel is determined by the thickness of the gaskets after tightening the two flanges and is found to be 3.4 mm. The obstruction in the flow path due to the wires promotes localized turbulence. The same set up is used for NF as well as RO using suitable membranes. The schematic of the experimental setup is available elsewhere [16].

Operating Conditions

Pretreatment

Eight alum dosages, namely, 0.1, 0.2, 0.3, 0.5, 1, 2, 3 and 5% (weight by volume) are used to obtain the optimum alum concentration.

Membrane experiments:

Ultrafiltration:

Ultrafiltration experiments are conducted at three different pressures of 276, 414, and 552 kPa with cross flow velocities of 0.1 m/s (Re=680), 0.15 m/s (Re=1020) and 0.2 m/s (Re=1360) in laminar regime both with and without promoter. In turbulent flow regime, ultrafiltration experiments are conducted at three different operating pressures of 759, 828 and 897 kPa. At 759 kPa, experiments are carried out at Reynolds numbers of 4762, 5442 and 6122, whereas at 828 and 897 kPa experiments are conducted at a Reynolds number of 4762 only.

Nanofiltration:

Nanofiltration studies are conducted at three pressures (828, 966, 1104 kPa) with cross flow velocities of 0.1 m/s (Re=680), 0.15 m/s (Re=1020) and 0.2 m/s (Re=1360) in laminar regime both with and without promoter. Cross flow velocities of 0.7 m/s (Re=4762), 0.8 m/s (Re=5442) and 0.9 m/s (Re=6122) are used in turbulent regime.

Table 1. Characterization of effluent.

	pH	Conductivity $\times 10^{-1}$ (s/m)	TS (g/l)	TDS (g/l)	COD (ppm)	BOD (ppm)	Cl ⁻ (ppm)	Ca ⁺⁺ (ppm)
Feed	10.4	56.1	46.6	36.9	8120	3123	15200	400
After pretreatment	7.25	24	44.3	15.9	2732	1050.8	15200	380

Experimental procedure

Pretreatment

Pretreatment of the effluent is carried out in 50 ml graduated cylinder with different dosages of alum for twenty four hours. It may be pointed out that the rate of coagulation remains almost unchanged beyond half an hour. The optimum alum dose is established by examining various properties (*e.g.*, pH, TDS, conductivity, TS, COD, turbidity) of supernatant solutions. The effluent is subjected to coagulation at optimum alum dosing in a 40 l bucket. The sludge produced is sun dried and pulverized to powder form and stored.

Membrane experiments:

The steps used in the experiments are as follows:

- 1. Compaction of membranes:* A fresh membrane is compacted at a pressure higher than its operating pressure for three hours using distilled water.
- 2. Determination of membrane permeability:* Membrane permeability is determined using distilled water. Flux values at various operating pressures are measured and the slope of flux versus pressure plot gives the permeability.
- 3. Conduction of the experiments:* The effluent is placed in a stainless steel feed tank of 10 l capacity. A high pressure plunger pump is used to feed the effluent into the cross-flow membrane cell. The retentate stream is recycled to the feed tank routed through a rotameter. The permeate stream is also recycled to maintain a constant concentration in the feed tank. A bypass line from the pump delivery to the feed tank is provided. The two valves in the bypass and the retentate lines are used to vary the pressure and the flow rate through the cell, independently. Cumulative volumes of permeate are collected during the experiment and the duration of the each experiment is one hour. Values of permeate flux are determined from the slopes of cumulative volume versus time plot. Permeate samples are collected at different times for analysis. Among 50 experiments (including UF and NF), about 25 experiments are repeated three times and the typical standard deviation value for the experimental permeate flux is $0.032 \times 10^{-6} \text{ m}^3/\text{m}^2\text{s}$.
- 4. Determination of new permeability:* Once an experimental run is over, the membrane is thoroughly washed, in situ, with distilled water for fifteen minutes applying a maximum pressure of 200 kPa. The cross-flow channel is then dismantled and the membrane is dipped in 0.12 (N) hydrochloric acid solution for three hours. Next, it is washed carefully with distilled water to remove traces of acid. The cross-flow cell is reassembled and the membrane permeability is again measured. It is observed that the membrane permeability remains almost constant between successive runs.

Sequence of the experiments: The sequences of experiments are: a) pretreatment of the effluent by alum; b) ultrafiltration of pretreated effluent; c) nanofiltration. Feed for nanofiltration is obtained by collecting permeate from ultrafiltration at 828 kPa and Reynolds number 4762. This experimental scheme is shown in Figure 1.

Analysis

Calcium and chloride present in various samples are estimated by Orion Aplus™ Benchtop Ion Meter (supplied by M/s, Thermo Electron Corporation, Beverly, MA, U.S.A.) using ion specific electrodes. COD and BOD values of each stream are measured by standard techniques [21]. The conductivities and TDS of all the streams are measured by an auto ranging conductivity meter (Chemito 130 manufactured by Toshniwal Instruments, India). pH of the samples are measured by a pH meter, supplied by Toshniwal Instruments, India. Total solids (TS) of all the samples are measured by weighing a known volume of sample in a petri dish and keeping it in a vacuum oven maintained at $105 \pm 2^\circ \text{C}$, till complete drying of the sample. The powdered form of the sludge from coagulation is analyzed for its fertilizer value. The samples are sent for analysis to Agronomy Laboratory of The Agriculture and Food Engineering Department, Indian Institute of Technology, Kharagpur.

Results and Discussion

Pretreatment

The effluent is tested for optimum alum dosing for coagulation. It is observed that beyond an alum concentration of 2%, TDS, conductivity and TS concentration increase significantly. The COD of the clarified liquor decreases with alum concentration and beyond 2%, the change is gradual. It may also be noted that with increasing concentration of alum, the turbidity of the solution decreases (with more settling of solids) sharply and beyond 2%, the decrease is gradual. It is also observed that the pH of the clear solution is close to the normal pH (~ 7.25) at 2% alum concentration and it decreases further with increase in alum dose. From these observations, 2% is selected as the optimum concentration of alum for coagulation. The clarified liquor after optimum alum dosing is subjected to membrane filtration after filtering using a fine cloth. The dried and pulverized sludge is analyzed for its fertilizer value (pH: 6.6; Organic Carbon (wt%): 10.5; Nitrogen (wt%): 1.55; Phosphorous (wt%): 0.074; Potassium (wt%): 0.5) and is compared with vermi compost (pH: 7.1-7.8; Organic Carbon (wt%): 9.97-10.62; Nitrogen (wt%): 1.80; Phosphorous (wt%): 0.90; Potassium (wt%): 0.4). It is observed that the properties of the sludge are close to those of vermi compost. Therefore, the sludge produced (1.1 kg from 40 liters of effluent) can be used as a good fertilizer.

Ultrafiltration

Transient flux decline

Figures 2 and 3 represent the flux decline behavior of the effluent in turbulent and laminar flow regime, respectively. It can be seen from the figures that the time required to reach steady state decreases with increase in Reynolds number. Fig. 2 shows that the steady state is attained in about 256 s, for Re=4762 and 759 kPa pressure, whereas at Re=5442 and Re=6122, the steady states are attained within 210 s and 179 s, respectively at the same transmembrane pressure. As shown in Figure 2, the flux decline is about 21% of the initial value for Re=4762, about 19% with for Re= 5442, and 16 % for Re=6122. As Reynolds number increases, the growth of the polarized layer over the membrane surface decreases due to enhanced forced convection and steady state is attained at an earlier time. The resistance to the solvent flux also decreases with increase in cross flow velocity and permeate flux increases. Hence, the flux decline is lower at

higher cross flow velocities. On the other hand, steady state is attained faster with an increase in operating pressure at a fixed cross flow velocity. For example, in Figure 2, for Re=4762, steady states are attained in about 218 s and 181 s respectively for 828 and 897 kPa pressures. Whereas at the same Re=4762, time required to attain steady state is about 210 s for an operating pressure of 759 kPa. Steady state is achieved faster using turbulent promoter compared to laminar flow. It can be observed from Figure 3 that at Re=680 and 276 kPa, the steady state is attained in about 1025 s without promoter and about 813 s with promoter at the same operating condition. The flux decline is about 34 % without promoter at Re=680 and 276 kPa pressure; but only 28 % using promoter at the same operating condition. Turbulent promoters generate local turbulence and hence reduce the concentration polarization at the membrane surface. Steady state is established faster than without promoter as the growth of the polarized layer is controlled quickly. Therefore, the flux decline is also lower compared to the purely laminar flow condition.

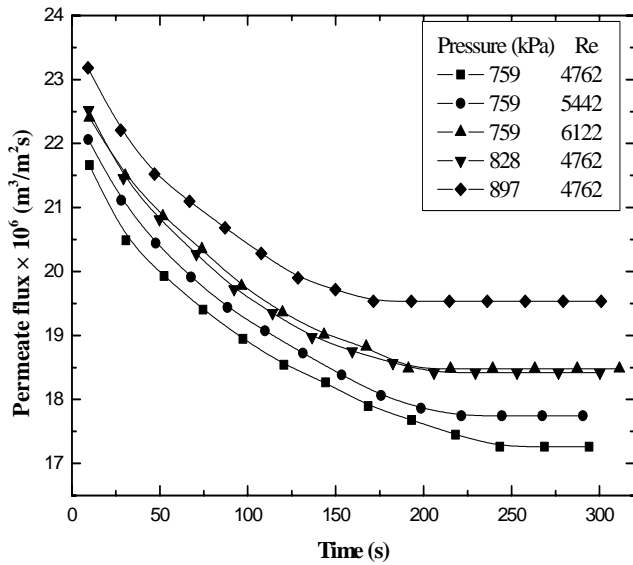


Figure 2. Transient flux decline of Turbulent flow regime in UF.

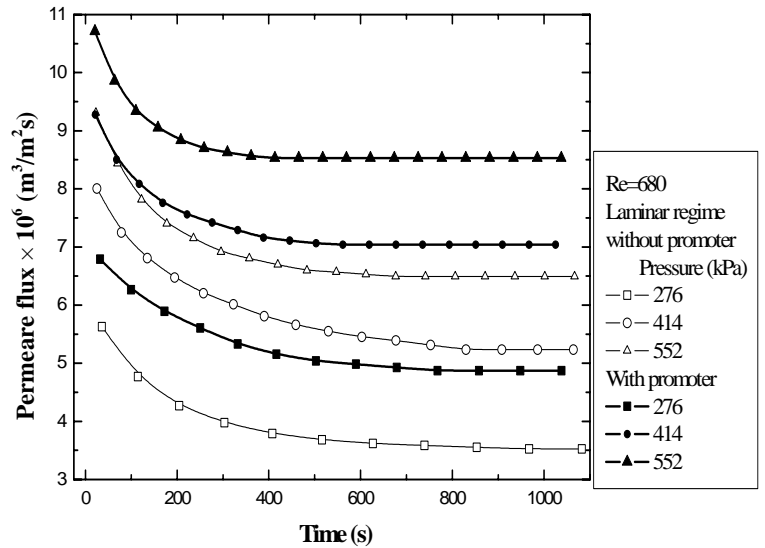


Figure 3. Transient flux decline of Laminar flow regime in UF.

Steady state

The variations of steady state permeate flux with pressure at different Reynolds number under turbulent flow, laminar flow without and with turbulent promoters are shown in Figure 4. The figure shows the usual trend that the permeate flux increases with operating pressure and Reynolds number, as expected. Higher flux is achieved at higher pressure due to increase in driving force. The increase in flux with Reynolds number is due to reduction in concentration polarization as discussed earlier. The percentage enhancements of the permeate flux in laminar regime with turbulent promoters for all the operating conditions are 27 to 38%. All the increases are calculated taking the laminar flow results under same operating conditions as the basis. The formation of polarized layer over the membrane surface is significantly reduced in presence of the turbulent promoters. This causes a corresponding increase in permeate flux.

Analysis of polarized layer resistance

From the steady state flux values obtained from the experimental results, the polarized layer resistance at the steady state is calculated as,

$$R_p^s = \frac{\Delta P}{\mu V_w^s} - R_m \quad (5)$$

for various operating conditions. The variation of non-dimensional steady state polarized layer resistance with Reynolds number is presented in Figure 5, for all the hydrodynamic conditions.

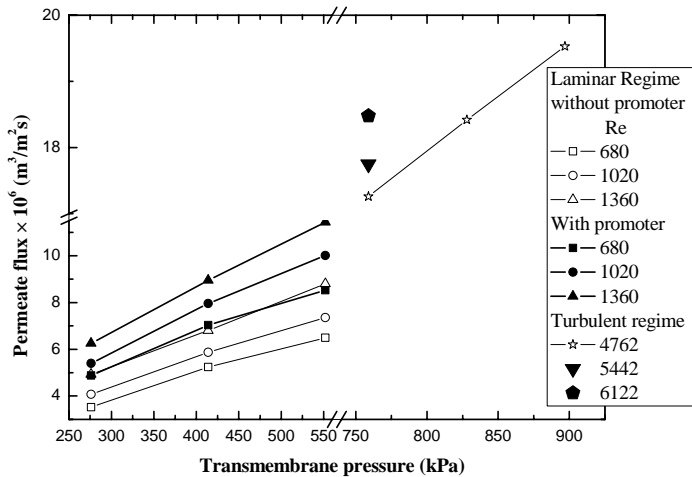


Figure 4. Variation of permeate flux with pressure drop in UF.

It is observed from the figure that the steady state values of R_p decreases with Reynolds number as expected. For example, for a transmembrane pressure drop of 552 kPa in laminar flow, the ratio of the polarized layer and hydraulic resistance reduces from 2.3 to 1.5 with an increase in Reynolds number from 680 to 1020. R_p values increase with the transmembrane pressure drop. With increase in pressure, more solutes are convected towards the membrane and this enhances the concentration polarization, resulting in increase in R_p values. For the case with the promoters, the polarized layer resistance decreases significantly due to the enhanced turbulence near the membrane surface induced by the promoters. At the same Reynolds number (680) and transmembrane pressure (552 kPa), the presence of turbulent promoters reduces the resistance to 1.5 compared to 2.3 in laminar flow. This reduction in R_p^s is more than 41% in some of the experiments leading to a significant enhancement of the permeate flux. The figure also shows further reductions in the polarized layer resistance for the case of purely turbulent flows. The steady state polarized layer resistance is correlated with the operating pressure and Reynolds number as,

$$\frac{R_p^s}{R_m} = a \left(\frac{\Delta P}{\Delta P_{\max}} \right)^{n1} (\text{Re})^{n2} \quad (6)$$

where ΔP_{\max} is the maximum transmembrane pressure (897 kPa for UF and 1104 kPa for NF experiments).

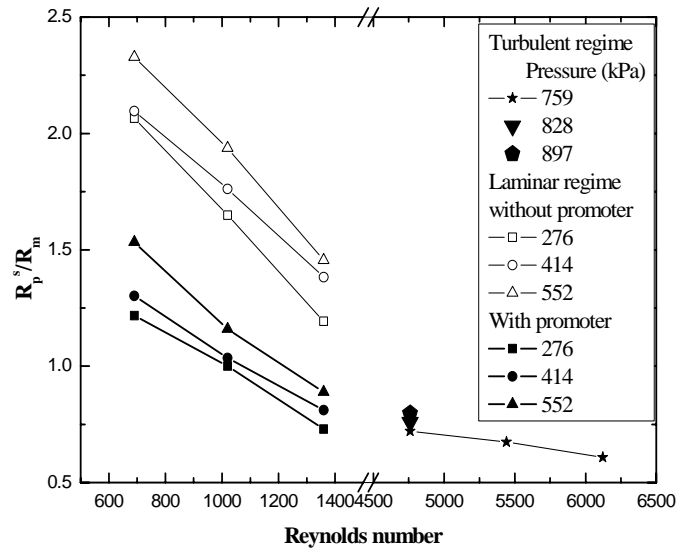


Figure 5. Variation of the ratio of polarized layer and hydraulic resistances at steady state with Reynolds number during UF.

The values of $\ln a$, n_1 , n_2 are evaluated using non linear regression and are presented in Table 2 for different hydrodynamic conditions. The positive values of n_1 and negative values of n_2 confirm the trend of polarized layer resistance with the operating conditions as discussed earlier. It may be observed from Figure 5 that Reynolds number has a significant effect on the polarized layer resistance. For laminar flow with and without promoter, polarized layer resistance is the major contributing resistance. For example, in case of pure laminar flow, at Reynolds number=1360 and transmembrane pressure drop at 552 kPa, R_m and R_p constitute about 30% and 70% of the total resistance, respectively. In case of laminar flow with promoter, at the same operating condition, contribution of R_p decreases to 61% of the total resistance. For turbulent flow regime, effects of Reynolds number are really profound and polarized layer resistance becomes comparable to the membrane hydraulic resistance. For the range of Reynolds number studied herein, R_p^s varies between 0.6 to 0.8 times of R_m . At Reynolds number =4762, R_p contributes about 42% of total resistance, whereas, at Reynolds number =6122, it is about 38%.

The values of R_p^s at different operating conditions are evaluated from correlation presented in Eq. (6). Now, with these R_p^s values and experimentally observed R_p values,

$$\ln\left(\frac{R_p^s}{R_p^s - R_p}\right)$$

is plotted at various time points for a fixed set of operating conditions, resulting into almost straight line through origin. The slope of these curves estimates the value of 'k' which is the kinetic rate constant of the growth of polarized layer resistance. For laminar flow without promoter, the range of 'k' is 0.004 s⁻¹ to 0.01 s⁻¹; for laminar flow with promoter it is from 0.006 s⁻¹ to 0.019 s⁻¹ and for turbulent flow it is from 0.015s⁻¹ to 0.026 s⁻¹. The parameter 'k' has a major role in the rate of the growth of polarized layer resistance, as observed in the following equation,

$$\frac{dR_p}{dt} = R_p^s \frac{k}{\exp(kt)} \quad (7)$$

The exponential term involving 'k' in the denominator of the above equation has more influence in determining the value of the slope of R_p curve (i.e. $\frac{dR_p}{dt}$). It may be

observed from Figure 6 that the rate of growth of polarized layer resistance (hence permeate flux, refer Figures 2 and 3) is a function of the operating conditions. Therefore, the parameter 'k' is correlated with non-dimensional pressure drop and Reynolds number as,

$$k = b \left(\frac{\Delta P}{\Delta P_{\max}} \right)^{m_1} (\text{Re})^{m_2} \quad (8)$$

The model constants $\ln b$, m_1 and m_2 are evaluated using non linear regression and are presented in Table 3 for different hydrodynamic conditions. Using regressed 'k' values and Eq. (6) for R_p^s , the profiles of R_p are calculated and are presented in Figure 6 for various operating conditions. It may be observed from Table 3 that the values of the parameters m_1 and m_2 are always positive indicating increase in 'k' with the operating pressure and Reynolds number. Interestingly, it may also be observed from this table that the values of the parameters m_1 and m_2 are in increasing order for laminar, laminar with promoter and turbulent flow conditions. This physically indicates

that the values of $\frac{dR_p}{dt}$ is less for laminar, laminar with promoter and turbulent flow, in that order. Hence, the attainment of steady state is earliest for turbulent flow and is gradual for laminar flow without promoter. This trend can be confirmed from Figure 6. It may also be noted that since 'k' increases with operating pressure and Reynolds number, the rate of growth of the polarized layer resistance is less at higher transmembrane drop and Reynolds number. This indicates an early onset of the steady state for higher operating pressure and Reynolds number (refer Figure 4). It is observed from Figure 6 that the calculated profiles of R_p match closely with the experimental values. For all the hydrodynamic conditions, the R_p values are lower at higher Reynolds number as expected.

Table 2. Model constants for R_p^s/R_m .

Operating condition		$\ln a$	n_1	n_2	r^2
Ultrafiltration	Turbulent	5.47±0.45	0.56±0.004	-0.67±0.005	0.99
	Laminar	5.28±0.28	0.23±0.004	-0.68±0.007	0.95
	Laminar with promoter	5.14±0.25	0.27±0.004	-0.73±0.007	0.97
Nanofiltration	Turbulent	10.73±0.75	0.34±0.004	-1.25±0.006	0.96
	Laminar	3.73±0.14	0.27±0.003	-0.39±0.007	0.96
	Laminar with promoter	2.52±0.19	0.50±0.004	-0.30±0.007	0.95

Permeate quality

The permeate quality after UF, for various operating conditions, is presented in Table 4. The conductivity of the permeate is slightly less compared to the feed which signifies that about 88% of the salt present in the feed solution has permeated through the UF membrane. Variations of permeate COD with trans-membrane pressure at the operating Reynolds number in turbulent, laminar and with turbulent promoter are shown in Figure 7. With increase in pressure drop the permeate quality in terms of COD increases and with Reynolds number, it decreases. With increase in pressure, the solvent flux as well as solute flux increase linearly and thus COD of the

permeate increases. As Reynolds number increases, the growth of the polarized layer over the membrane surface is reduced due to enhanced forced convection as discussed earlier. So the solute concentration of the permeate and as a result of which COD decreases. It can be observed from Figure 7 that at 276 kPa pressure and Re=680, COD is 440 where as at 552 kPa pressure and at same Re, the COD is 472. It is also observed that at 276 kPa pressure and Re=680, COD decreases by about 3% in presence of promoter. At Re=4762, as the transmembrane pressure increases from 759 kPa to 897 kPa, COD increases by 8%. For a transmembrane pressure drop of 759 kPa, COD reduces from 512 to 400 with an increase in Reynolds number from 4762 to 6122.

Table 3. Model constants for k.

Operating condition		<i>lnb</i>	<i>m</i> ₁	<i>m</i> ₂	<i>r</i> ²
Ultrafiltration	Turbulent	-21±1.42	3.55±0.004	2.05±0.006	0.94
	Laminar	-8.92±0.67	0.61±0.004	0.50±0.008	0.93
	Laminar with promoter	-7.44±0.56	1.12±0.004	0.58±0.008	0.92
Nanofiltration	Turbulent	-13.04±0.78	2.84±0.004	1.10±0.006	0.99
	Laminar	-8.42±0.59	1.77±0.004	0.56±0.008	0.95
	Laminar with promoter	-7.97±0.55	2.09±0.004	0.59±0.008	0.90

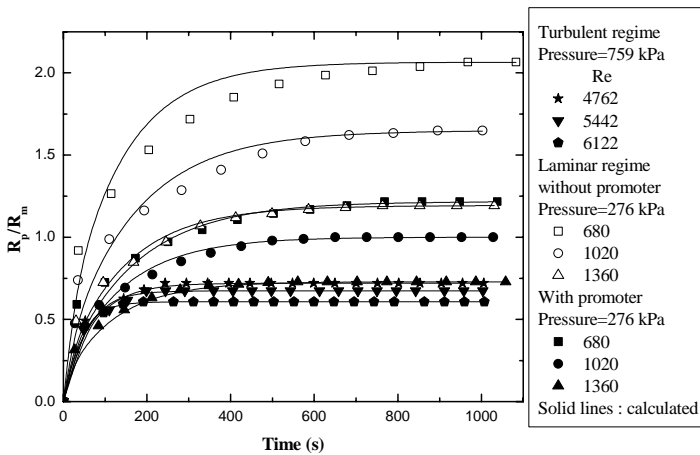


Figure 6. Variation of calculated dimensionless polarized layer resistance with time in UF.

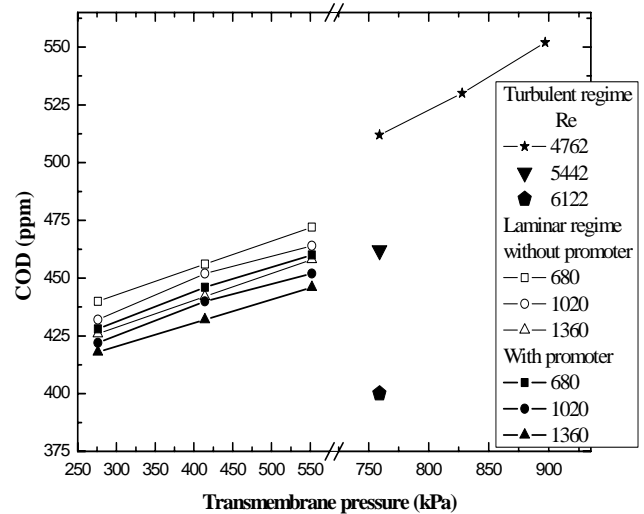


Figure 7. Variation of COD with pressure drop in UF.

Table 4. Permeate analysis after ultrafiltration.

Sr. No	Pressure	Reynolds	TDS	TS	pH	Conductivity ×	Cl ⁻	Ca ⁺⁺	BOD
	kPa	number	ppm	ppm		10 ⁻¹ (S/m)	ppm	ppm	ppm
Turbulent regime									
1	759	4762	13200	31100	7.68	20.2	13600	320	142.2
2	759	5442	13200	30300	8.01	20.0	13420	310	128.3
3	759	6122	13000	29500	7.98	19.7	13200	300	111.1
4	828	4762	13300	32700	7.63	20.4	13800	340	147.2
5	897	4762	13500	33200	7.90	20.7	14100	342	153.3
Laminar regime									
1	276	680	13700	27100	7.76	21.1	12430	280	122.2
2	276	1020	13500	26600	7.81	20.8	12540	280	120.0
3	276	1360	13300	26000	7.78	20.5	12630	290	118.3
4	414	680	14000	28300	7.81	21.6	12620	290	126.7
5	414	1020	13800	27500	7.81	21.3	12720	300	125.6
6	414	1360	13700	27000	7.50	21.1	12830	310	122.8
7	552	680	14400	29400	7.64	22.2	12790	300	131.1
8	552	1020	14300	28700	7.72	22.0	12850	320	128.9
9	552	1360	13900	28000	7.79	21.4	12920	320	127.2
With turbulent promoter									
1	276	680	13300	26000	7.50	20.5	12390	270	118.9
2	276	1020	13400	25800	7.59	20.6	12490	280	117.2
3	276	1360	13100	25800	7.51	20.1	12600	300	116.1
4	414	680	13700	27600	7.51	21.0	12580	280	123.9
5	414	1020	13500	27200	7.47	20.8	12670	290	122.2
6	414	1360	13400	27000	7.58	20.6	12780	300	120.0
7	552	680	14100	28800	7.49	21.7	12730	290	127.8
8	552	1020	13900	28100	7.51	21.3	12800	300	125.6
9	552	1360	13700	27600	7.53	21.0	12870	300	123.9

Nanofiltration

Transient flux decline

Figure 8 represents the flux decline behavior of the effluent at 828 kPa pressure. It can be clearly seen from the figure that the time required to reach steady state decreases with increase in Reynolds number. For example, it can be observed from Figure 8 that the steady state is attained in about 430 s, for $Re=4762$ and 828 kPa pressure, whereas at the same pressure but at $Re=5442$ and $Re=6122$, the steady states are attained within 384 s and 330 s, respectively. The flux decline is about 22% of the initial value for $Re=4762$, about 20% with increase in $Re=5442$, and 18 % at $Re=6122$. Similar trends can be observed for flux decline in laminar regime with and without promoters. As the cross flow velocity increases, the growth of the polarized layer over the membrane surface is arrested faster because of enhanced forced convection. This leads to the onset of steady state at an earlier time. For the above reason, the resistance to the solvent flux also decreases with the cross flow velocity, resulting in higher permeate flux. Therefore, the flux decline is lower at higher cross flow velocities. It is also observed that the steady state is achieved faster using turbulent promoter compared to laminar flow. For example, in Figure 8, at $Re=680$ and 828 kPa, the steady state is attained in about 939 s without promoter and about 579 s with promoter at the same operating condition. The flux decline is about 31 % without promoter at $Re=680$ and 828 kPa pressure; but only 20.5 % using promoter at the same operating condition. Use of the turbulent promoters creates local turbulence, thus reducing the

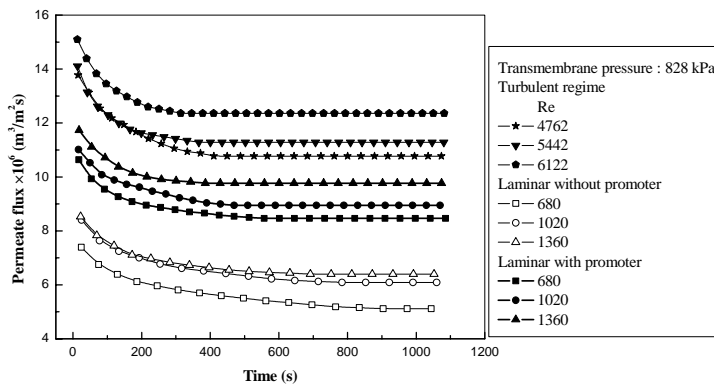


Figure 8. Transient flux at 828 kPa pressure in NF.

concentration polarization at the membrane surface and the growth of the polarized layer is controlled quickly, establishing steady state earlier than without promoter. Since the concentration polarization is reduced due to the presence of the promoters, the flux decline is also less compared to the no promoter case. As shown in Figure 8, at 828 kPa and Reynolds number 680, the steady state flux enhancement is 52.8%, whereas, at Reynolds number of 1020 and 1360, the corresponding steady state flux enhancement values are 47% and 65%, respectively. It may be mentioned here that at 966 kPa pressure, the flux enhancement using promoters is in the range of 47% to 60% for the operating range of Reynolds number (680 to 1360). For 1104 kPa pressure, this range is in between 45 to 58%. These data indicates that the percentage flux enhancement using promoters is almost invariant with respect to the operating conditions (*i.e.*, transmembrane pressure drop and Reynolds number).

Steady state flux

The variations of steady state permeate flux with pressure at different Reynolds number under turbulent flow, laminar flow without and with turbulent promoters are shown in Figure 9. The figure shows the usual trend that the permeate flux increases with operating pressure and Reynolds number. Higher flux at higher pressure is due to enhanced driving force. The increase in flux with Reynolds number is because of decreasing concentration polarization as discussed earlier. It may be noted here that the variation of permeate flux with pressure at various Reynolds number in NF experiments is different from the UF runs (Figures 4 and 9).

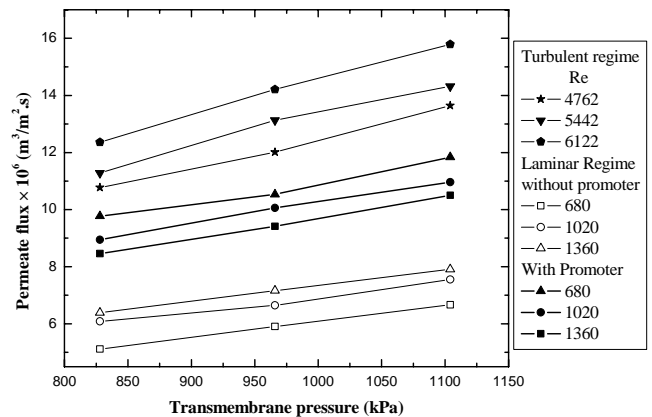


Figure 9. Variation of permeate flux with pressure drop in NF.

The increase in flux values is more with the transmembrane pressure in UF (Figure 4) compared to Figure 9. For example, at $Re=1360$ (without promoter), the flux increase from $4.9 \times 10^{-6} \text{ m}^3/\text{m}^2\text{s}$ to about $8.8 \times 10^{-6} \text{ m}^3/\text{m}^2\text{s}$ when the transmembrane pressure increases from 276 to 552 kPa, indicating about 80% increase. Under the same Reynolds number, in case of NF, flux enhancement is only 27% when pressure increases from 828 to 1104 kPa. Similar trend is observed for other operating conditions, as well. These results indicate that the deposition over the membrane surface is more compact in case of NF. The organic materials permeated through UF form a compact cake type layer over the NF membrane. Hence, the flux enhancement by pressure and cross flow velocity is less in case of NF. The percentage enhancements of the permeate flux in laminar regime with turbulent promoters for all the operating conditions are in the range of 45 to 66%. All the increases are calculated taking the laminar flow results under same operating conditions as the basis. The formation of polarized layer over the membrane surface is significantly reduced in presence of the turbulent promoters. This causes a corresponding increase in permeate flux. It may be noted here that flux enhancement in NF with turbulent promoter is more (45 to 66%) compared to that in UF (27 to 38%). This indicates that the deposition over the membrane surface is much less sticky in case of NF, constituting mainly the lower molecular weight organic materials and inorganic substances. The results for turbulent flow regime cannot be directly compared to the laminar flow results for flux enhancement calculations, as the operating conditions are different. However, it can be clearly seen from Figure 9 that the permeate flux in turbulent flow at a specific pressure is considerably higher than either the laminar or the turbulent promoter enhanced cases.

Analysis of polarized layer resistance

Figure 10 represents the variation of non-dimensional

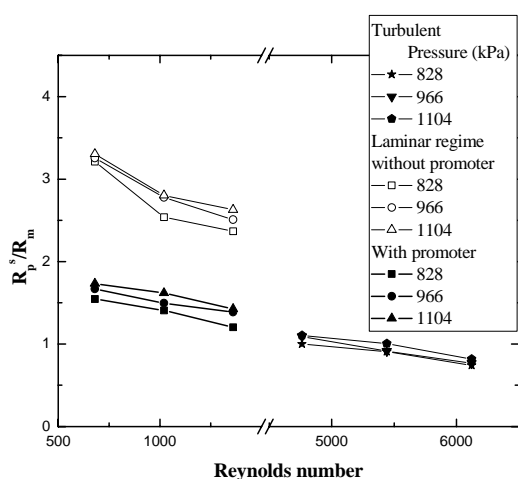


Figure 10. Variation of the ratio of polarized layer and hydraulic resistances at steady state with transmembrane pressure in NF.

steady state polarized layer resistance with transmembrane pressure drop, for all the hydrodynamic conditions. The steady state values of R_p increase marginally with the transmembrane pressure drop and decrease significantly with increase in Reynolds number as discussed earlier. For example, the dimensionless polarized layer resistance increases from 2.5 to 2.8 when pressure increases from 828 to 1104 kPa, at $Re=1020$. Increase in polarized layer resistances is marginal with pressure for laminar flow with promoter and for all cases of turbulent Reynolds numbers. This clearly indicates that the polarized layer is almost incompressible within the pressure range studied here. Presence of turbulent promoters reduces the polarized layer resistance. For example, at 966 kPa pressure and $Re=1020$, polarized layer resistance decreases by about 46%, when promoters are introduced. Under turbulent flow conditions, effect of Reynolds number is more marked on the polarized layer resistance. For example, for all the operating pressure values, polarized layer resistance varies from 0.7 to 1.1, which are significantly less compared to those under laminar flow conditions (2.4 to 3.3) and under laminar flow with promoter (1.2 to 1.7). At 828 kPa pressure, R_p/R_m value decreases by about 26% when Reynolds number increases from 4762 to 6122. Under turbulent conditions, polarized layer resistance becomes comparable to the membrane hydraulic resistance. At 828 kPa pressure, it contributes about 50% to the total resistance. Contribution of polarized layer resistance is about 49% with promoter and is about 73% without promoter (under laminar flow condition) at the same operating pressure level.

For various flow regimes, the R_p^s/R_m and ' k ' values are fitted with the operating conditions as given in Eqs. (6) and (8) and the estimated parameters are tabulated in Table 2 and 3 respectively. The calculated and experimental R_p values are presented in Figure 11 for all operating conditions. Figure 11 shows a close match between the calculated and experimental data.

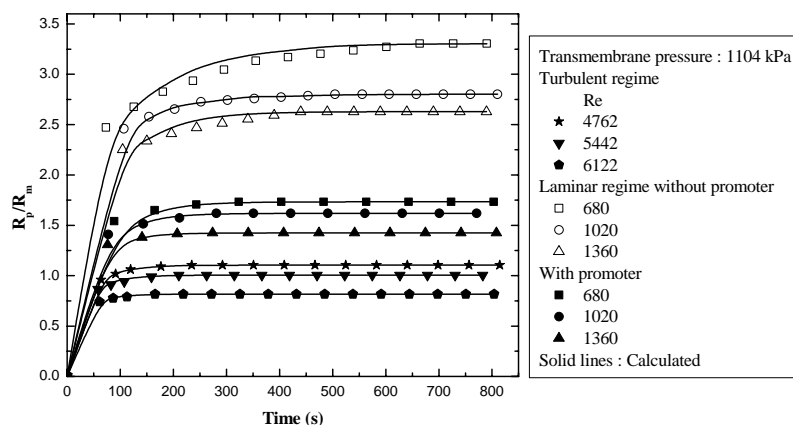


Figure 11. Variation of calculated dimensionless polarized layer resistance with time in NF.

Permeate quality

The permeate quality after NF, for various operating conditions, is presented in Table 5. Variations of permeate COD with trans-membrane pressure at the operating Reynolds number in turbulent, laminar and with turbulent promoter are shown in Figure 12. It is observed that with increase in pressure drop and Reynolds number, the permeate quality improves. With increase in pressure, the solvent flux increases linearly, while the solute flux is nearly independent of pressure for less open membranes (RO and in some cases for NF membranes) [22]. This indicates that with increasing pressure, more solvent passes through the membrane along with a fixed amount of the solute; the permeate becomes purer and hence the permeate quality (expressed as COD) increases. The similar trends are observed for laminar flow with promoter and turbulent flow. It can be seen from Figure 12 that at 828 kPa pressure and $Re=680$, COD decreases by about 23% in presence of promoter compared to the base case (laminar at same operating conditions). Percentage decrease in COD is found to be about 16% at 966 kPa pressure and $Re=1360$ and about 12% at 1104 kPa pressure and $Re=1360$. At $Re=4762$, as the transmembrane pressure increases from 828 kPa to 1104 kPa, COD decreases by 30%.

Conclusion

Effluent from a delimiting-bating unit has been successfully treated using a combined process of coagulation by alum and membrane separation processes consisting of UF followed by NF. The optimum alum dose is found to be 2 % (wt/vol). The time required to reach steady state decreases with increase in Reynolds number and applied pressure. The use of turbulent promoters in laminar regime results in substantial increase in flux (27-38% for UF and 45-66% for NF) compared to the laminar case. Both in UF and NF, polarization resistance is the major contributor to overall resistance to the solvent flow (70% for UF and 77% for NF). A first order kinetic model adequately describes the growth rate of polarized layer resistance. Increase of permeate flux with transmembrane pressure is more pronounced in UF (77-85%) compared to NF (20-34%). The retentate of the NF can be recycled to bating process and permeate can be used as wash water. The sun dried sludges obtained from process can be used as organic fertilizer. The COD (~92 ppm) and BOD (~25 ppm) values in the permeate of NF are well below the discharge limit of the same.

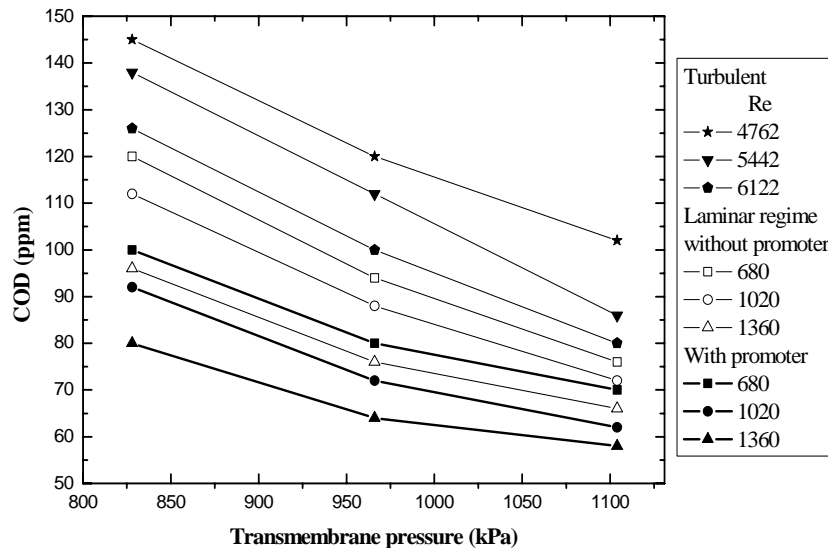


Figure 12. Variation of COD with pressure drop in NF.

Table 5. Permeate analysis after nanofiltration.

Sr.No	Reynolds	Pressure	TDS	TS	pH	Conductivity	Ca ⁺⁺	Cl ⁻	BOD
	number	kPa	Ppm	ppm		× 10 ⁻¹ (S/m)	ppm	ppm	ppm
Turbulent regime									
1	4762	828	8690	17900	7.94	13.2	11080	220	40.3
2	5442	828	8870	18100	8.00	13.4	11040	210	38.3
3	6122	828	8610	17500	8.04	13.0	11010	205	35.0
4	4762	966	9860	17000	7.98	14.9	11000	210	33.3
5	5442	966	6870	17300	7.99	10.4	11010	200	31.1
6	6122	966	8500	16800	8.00	12.9	10980	195	26.7
7	4762	1104	8640	16700	7.98	13.1	10960	200	28.3
8	5442	1104	8490	16700	7.90	12.9	11000	210	23.9
9	6122	1104	8910	16400	7.97	13.4	10980	190	22.2
Laminar regime									
1	680	828	9400	19500	8.11	14.8	10960	200	34.4
2	1020	828	9100	19100	7.99	14.5	10960	205	31.1
3	1360	828	9150	18900	7.93	14.3	10920	190	26.7
4	680	966	9200	18800	7.95	14.4	10900	195	25.0
5	1020	966	8170	18300	7.84	14.0	10860	190	22.8
6	1360	966	8310	18000	7.78	13.5	10860	195	21.1
7	680	1104	8600	17700	7.90	13.4	10880	185	22.2
8	1020	1104	8830	17200	7.71	13.1	10840	180	20.0
9	1360	1104	9180	16500	7.74	12.8	10800	180	18.3
With turbulent promoter									
1	680	828	9080	19000	7.92	14.2	11010	195	26.7
2	1020	828	9010	18700	8.01	13.8	10920	190	25.6
3	1360	828	8870	18200	8.00	13.8	10900	180	22.2
4	680	966	8800	18300	7.74	13.9	10860	190	22.2
5	1020	966	8720	18000	7.62	12.4	10800	195	20.0
6	1360	966	8670	17600	7.51	12.6	10840	180	17.8
7	680	1104	8680	17100	7.52	13.0	10800	180	19.4
8	1020	1104	8600	16900	7.78	13.4	10780	185	17.2
9	1360	828	8540	16900	7.70	13.9	10800	180	16.1

Acknowledgements

This work is partially supported by a grant from the Department of Science and Technology, New Delhi, Government of India under the scheme no. DST/TSG/WM/2005 /55. Any opinions, findings and conclusions expressed in this paper are those of the authors and do not necessarily reflect the views of DST.

References

1. Datta, S. S. An introduction to the principles of leather manufacture, 4th Edition, Indian Leather Technologists' Association.
2. Purkait, M. K., Bhattacharya, P. K., De, S. (2005) Membrane filtration of leather plant effluent: Flux decline mechanism. *J Membr Sci*; 258: 85-96.
3. Espantaleón, A. G., Nieto, J. A., Fernández, M., Marsal, A. (2003) Use of activated clays in the removal of dyes and surfactants from tannery waste waters. *Appl Clay Sci*; 24: 105-110.
4. Scholz, W., Bowden, W. (1999) Application of membrane technology in the tanning industry. *Leather*; 201 (4694): 17–18.
5. Cassano, A., Molinari, R., Romano, M., Drioli, E. (2001) Treatment of aqueous effluents of the leather industry by membrane processes A review. *J. Membr Sci*; 181: 111-126.
6. Das, C., De, S., DasGupta, S. (2007) Treatment of liming effluent from tannery using membrane separation processes. *Sep Sci Technol*; 42:517-539.
7. Suthantharajan, R., Ravindranath, E., Chitra, K., Umamaheswari, B., Ramesh, T., Rajamani, S. (2004) Membrane application for recovery and reuse of water from treated tannery wastewater. *Desalination*; 164: 151-156.
8. Cassano, A., Adzet, J., Molinari, R., Buonomenna, M.G., Roig, J., Drioli, E. (2003) Membrane treatment by nanofiltration of exhausted vegetable tannin liquors from the leather industry. *Water Research*; 37: 2426–2434.
9. Cassano, A., Drioli, E., Molinari, R. (1997) Recovery and reuse of chemicals in unhairing, degreasing and chromium tanning processes by membranes. *Desalination*; 113: 251-261.
10. Drioli, E., Caggiano, R., Cammisa, C. (1982) Uno Studio Sull'introduzione dell' ultrafiltrazione nel processes di concia delle pelli. *Acqua Aria*; 4: pp. 391.
11. Ahmed, M. T., Taha, S., Chaabane, T., BenFarès, N., Brahimi, A., Maachi R., Dorange, G. (2005) Treatment of sulfides in tannery baths by nanofiltration. *Desalination*; 185: 269-274.
12. Cassano, A., Drioli, E., Molinari, R. (1998) Introduction to ultrafiltration into unhairing and degreasing operation. *J Soc Leather Technologists Chemists*; 82: 130-135.
13. Cassano, A., Criscuoli, A., Drioli E., Molinari, R. (1999) Clean operations in the tanning industry: aqueous degreasing coupled to ultrafiltration: experimental and theoretical analysis. *Clean Product processes*; 1 (4): 257-263.
14. Jain SK, Purkait MK, Bhattacharya PK, De S. (2006) Treatment of leather plant effluent by membrane separation processes, *Sep Sci Technol*; 41:3329-3348.
15. Ortega LM, Lebrun R, Noël IM, et al. (2005) Application of nanofiltration in the recovery of chromium (III) from tannery effluents. *Sep Purif Technol*; 44:45-52.
16. Das C, Patel P, De S, DasGupta S. (2006) Treatment of tanning effluent using nanofiltration followed by reverse osmosis. *Sep Purif Technol*;50:291-299.
17. Cassano A, Molinari R, Drioli E. (1999) Saving of water and chemicals in tanning industry by membrane processes. *Water Sci Technol*; 40:443-450.
18. Hafez A, Manharawy SE. (2004) Design and performance of the two-stage/two-pass RO membrane system for chromium removal from tannery wastewater. Part 3. *Desalination*;165:141-151.
19. Cassano, A., Drioli, E., Molinari, R., Bertolutti, C. (1996) Quality improvement of recycled chromium in the tanning operation by membrane processes. *Desalination*; 108: 193-203.
20. Pal, S., Swati, Ghosh, T.B., De, S., DasGupta, S. (2008) Optical evaluation of deposition thickness and measurement of permeate flux enhancement of synthetic fruit juice in presence of turbulence promoters. (Unpublished findings).
21. Trivedy, R. K., Goel, P. K. (1986) Chemical and biological methods for water pollution studies. Environmental Publications: Karad.
22. Bungay, P. M., Lonsdale, H. K., Pinho, M.N.de. (1983) Synthetic Membranes: Science, Engineering and Application. D. Reidel Publishing Company; pp312.